 doi:10.20944/preprints201806.0199.v1

Synthesis of Needle-like $BiVO_4$ with Improved Photocatalytic Activity under Visible Light Irradiation

Duy Trinh Nguyen and Seong-Soo Hong*

Department of Chemical Engineering, Pukyong National University, 365 Shinseonro, Busan, 48547, Korea

*Corresponding author : sshong@pknu.ac.kr

Abstract

A highly crystallized monoclinic-scheelite type $BiVO_4$ powders were successfully synthesized by solvothermal method. The as-synthesized $BiVO_4$ powders were characterized by XRD, FE-SEM, Raman spectroscopy, UV-vis DRS spectroscopy and TA-PL. From the XRD data and Raman spectra, the monoclinic-scheelite phase $BiVO_4$ sample can be obtained at higher solvothermal synthesis temperature more than 140 ^oC. The preparation conditions such as, the Bi/V molar ratio and synthesis temperature, have significantly effects on the morphologies of the $BiVO_4$ samples. BVO2 sample shows the highest PL peak, which has the highest formation rate of OH radicals and the highest photocatalytic activity. This result suggests that the formation rate of OH radicals shows a good correlation with the photocatalytic activity.

Keywords: needle-like $BiVO_4$, photodegradation of Rhodamine B, monoclinic-scheelite type $BiVO_4$

 doi:10.20944/preprints201806.0199.v1

1. Introduction

Recently, bismuth based complex oxides such as Bi_2MoO_6, $BiFeO_3$, $BiVO_4$, BiOCl, Bi_2WO_6 have much attention in field of photocatalysis because of their narrow band gap, chemically and thermally stable and nontoxic [1,2]. Among of them, $BiVO_4$ which is an effective photocatalyst for pollutant photodegradation and water splitting under visible-light irradiation [3] and carbon dioxide reduction has attracted increasing attention [4, 5]. It is well known that $BiVO_4$ powders have three crystal structure types: monoclinic scheelite (s-m $BiVO_4$), tetragonal zircon (z-t $BiVO_4$) and tetragonal scheelite (s-t $BiVO_4$) structure [6]. However, only s-m $BiVO_4$ shows the highest visible-light driven photocatalyst, which can be attributed to its electronic structure and optical properties. It possesses a narrow band gap (2.4 eV) due to the electronic excitation from a valence band by Bi 6s or a hybrid orbital of Bi 6s and O 2p to a conduction band of V 3d, allowing to the visible light absorption. However, the poor charge-transport characteristics and the weak surface adsorption properties lead to excessive electron-hole recombination, which limit its overall photocatalytic efficiency.

It is well known that shape, size, specific surface area, crystal structure and morphology of semiconductor photocatalysts play an important factor on their photocatalytic activity [7-9]. Thus, to enhance the photocatalytic activity of these semiconductor materials, their fabrication with controlling the morphology and crystal-facets have recently attracted considerable. For example, monoclinic structured $BiVO_4$ nanosheets with exposed {010} facets show a much higher photocatalytic activity than the bulk material for degradation of Rhodamine B under solar irradiation [10]. The monoclinic BiVO4 with a highly exposed (040) facet is assigned to be responsible for the high activity of O_2 evolution [11].

In this study, $BiVO_4$ powders were prepared by the solvothermal process using bismuth neodecanoate and ammonium metavanadate solutions as precursors and oleic acid as surfactant in water-ethanol media. $BiVO_4$ powders with different morphologies were selectively synthesized by

 doi:10.20944/preprints201806.0199.v1

adjusting the Bi/V molar ratio and preparation temperature. The properties of the as-synthesized $BiVO_4$ powders were investigated by XRD, FE-SEM, Raman spectroscopy, UV-vis DRS spectroscopy and TA-PL. We have also investigated whether the photocatalytic activity of these materials can bring about the decomposition of Rhodamine B (RhB) in the presence of visible light.

2. Experimental

Bismuth neodecanoate ($Bi(OCOC(CH_3)_2(CH_2)_5CH_3)_3$), ammonium metavanadate (NH_3VO_4, 99.996%), and oleic acid (OA, 90 %) were purchased from Sigma-Aldrich and were used as received without further purification. Ethanol (99.98 %) and water were of analytical grade and were purchased from Burdick & Jackson.

$BiVO_4$ materials with various morphologies were prepared using a solvothermal process. Typically, bismuth neodecanoate (5 mmol) was firstly added into the solution containing OA (50 mL) and ethanol (50 mL) under vigorous stirring for 30 min. The as-obtained solution was named as solution A. A proper amount of NH_3VO_4 (Bi/V molar ratios are adjusted to 1:1, 2:1, and 1:2 for the synthesis of BVO1, BVO2, and BVO3, respectively) was dissolved into 15 mL of 3 M NaOH aqueous solution and the as-obtained solution was named as solution B. Afterwards, solution B was added a drop wise into solution A. The mixture was stirred for 1 h before being transferred into a telfon-lined stainless steel autoclave and heated at 140 ^oC for 12 h. After each the reaction, the obtained suspension was centrifuged at 10000 rpm for 10 min. The obtained solids were washed with water and ethanol for several times and dried at 60 ^oC overnight, and followed by calcining at 300 ^oC for 3 h. We conducted experiments with temperature selected at 100 and 180 ^oC in order to examine the effect of synthesis temperature on the morphology of $BiVO_4$ prepared with Bi/V molar ratio=2/1. The as-prepared products were denoted as BVO4 and BVO5, respectively.

Preprints (www.preprints.org) | NOT PEER-REVIEWED | Posted: 12 June 2018 doi:10.20944/preprints201806.0199.v1

The crystal structures of $BiVO_4$ samples were examined by powder X-ray diffraction (XRD) patterns with Cu Kα radiation (λ = 1.5405 Å) in the 2θ range of 5-30 ° at a scan rate of 1.0 °/min (Rigaku Co. Model DMax). Raman spectra were recorded with Micro Raman spectrometer (Dongwoo Optron, MonoRa500i) in the range 200 to 1000 cm^{-1} with a laser beam of 785 nm. The morphology of the products was observed by scanning electron microscope (SEM, JEOL JSM6700F), which was operating at an accelerating voltage of 3 kV and equipped with an energy dispersive X-ray spectroscopy (EDS). The UV-vis diffuse reflectance spectrum (UV-vis DRS) of the products were recorded on a Varian Cary 100 using polytetrafluoroethylene (PTFE) as a standard. The indirect band gap energy (E_g) of all samples was calculated from the tangent line in the plots of the modified Kubelka–Munk function $[F(R'_\infty)h\vartheta]^{1/2}$ versus photon energy.

The formation of hydroxyl radicals (•OH) on the surface of photoirradiated BiVO4 sample is detected by photoluminescence (PL) technique using terephthalic acid as a probe molecule. Terephthalic acid readily reacts with OH radical generated from the visible illuminated catalyst surfaces to produce 2-hydroxyterephthalic acid (HTA) with a strong fluorescence characteristic peak. The PL peak intensity of HTA is in proportion to the amount of OH radicals produced in water [12,13]. The typical procedure was similar to those used for the photocatalytic decomposition of RhB, as shown above. A base aqueous solution (100 mL, TA = 5×10^{-4} M, and NaOH = 2×10^{-3} M) was added to the reactor instead of RhB. After 1h illuminated, 3 mL of the suspension was withdrawn and filtered through a 0.22μm membrane filter to get the clear solution. Fluorescence spectra were recorded on a Hitachi F-4500 fluorescence spectrophotometer (FL) using the 315 nm excitation light.

We calculated the photocatalytic activities of samples after performing photocatalytic decomposition of RhB under visible light using a 300W Xe-arc lamp (Oriel) and a 410 nm cut-off filter. The light was passed through a 10 cm thick IR water filter, and then it was focused onto a 150 mL Pyrex using a quartz window. The pH value of the solution was maintained at 7.0; the temperature of the solution was maintained within a range of 23–25 °C. To determine the catalytic

Preprints (www.preprints.org) | NOT PEER-REVIEWED | Posted: 12 June 2018 doi:10.20944/preprints201806.0199.v1

activity in these experiments, the reactor was filled with a mixture of RhB aqueous solution (10^{-5} M, 100 mL) and the given photocatalyst (100 mg). Before irradiation, the mixture was magnetically stirred in dark conditions for 60 minutes. Thus, we ensured an adsorption-desorption equilibrium between the surface of the photocatalyst and the organic molecules. At regular time intervals, we withdrew 3 mL of the suspension and filtered it through a 0.22 μm membrane filter to produce a clear solution. A decrease in the concentration of RhB solution was determined with a UV-visible spectrophotometer (Mecasys Optizen Pop) at λ = 554 nm.

3. Results and discussion

3.1. Characterization of $BiVO_4$ samples

Fig. 1 shows the XRD patterns of $BiVO_4$ samples, which were prepared using different Bi/V molar ratio(A) and different synthesis temperature(B). When $BiVO_4$ were prepared at the Bi/V molar ratio= 1/1 (BVO1) and 2/1 (BVO2), all the XRD peaks indexed well with the monoclinic phase of $BiVO_4$ (JCPDS 14-00688); the peaks appeared at $2\theta = 29^o$, while the splitting of peaks occurred at 18.5^o, 35^o, and 46^o, respectively, corresponding with the patterns reported earlier [14]. No peaks of any other phases or impurities were detected. When $BiVO_4$ were prepared at the Bi/V molar ratio= 1/2 (BVO3), however, the XRD peaks exhibited similar patterns to that of s-m $BiVO_4$ and showed coexistence of NaV_6O_{15} (JCPDS 24-1155) phase.

Preprints (www.preprints.org) | NOT PEER-REVIEWED | Posted: 12 June 2018 doi:10.20944/preprints201806.0199.v1

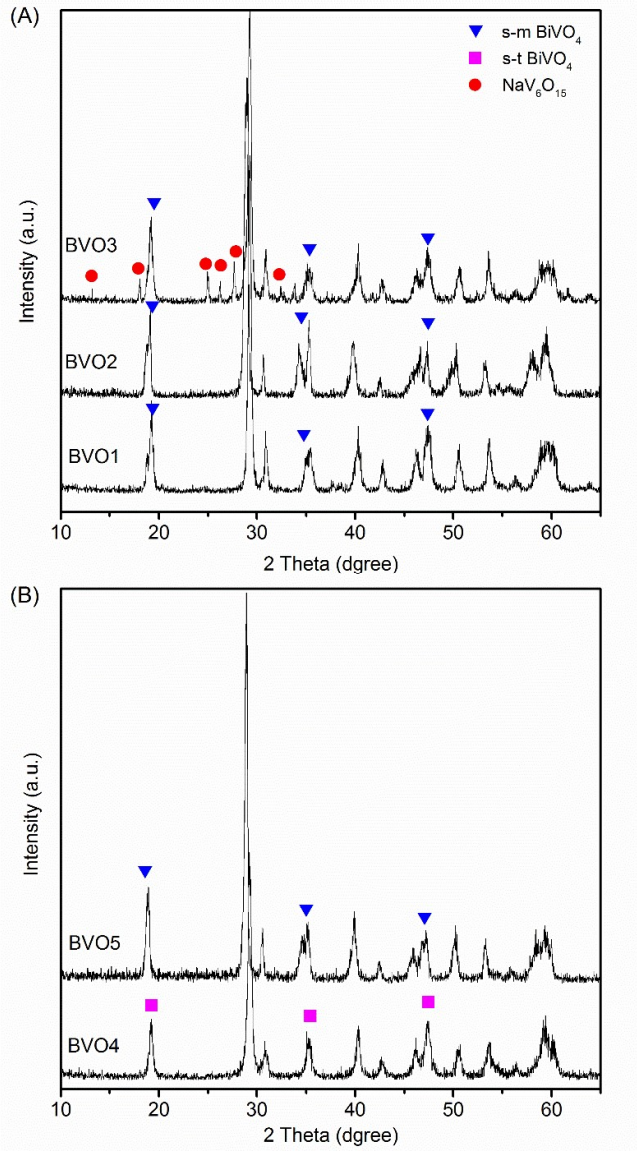

Fig. 1. XRD patterns of $BiVO_4$ samples prepared using different Bi/V molar ratio (A) and different synthesis temperature (B).

When $BiVO_4$ samples were prepared using different synthesis temperature, the XRD peaks showed the different patterns (Fig. 1B). When $BiVO_4$ samples were prepared at 100 ºC (BVO4), the XRD peaks indexed well with the tetragonal phase of $BiVO_4$ (JCPDS 14-00133) and no monoclinic phase of $BiVO_4$. However, all the XRD peaks indexed well with the monoclinic phase of $BiVO_4$ with an increase of synthesis temperature up to 140 and 180 ºC. This result indicated that the monoclinic phase of $BiVO_4$ samples could be obtained more than 140 ºC of solvothermal synthesis temperature.

Preprints (www.preprints.org) | NOT PEER-REVIEWED | Posted: 12 June 2018 doi:10.20944/preprints201806.0199.v1

Fig. 2 shows the Raman spectra of $BiVO_4$ samples, which were prepared using different Bi/V molar ratio(A) and different synthesis temperature(B). According to group theory, the monoclinic phase of $BiVO_4$ materials have six Raman-active modes: the external mode of $BiVO_4$ (210 cm^{-1}), the asymmetric deformation mode of VO_4^{3-} (324 cm^{-1}), the symmetric deformation mode of VO_4^{3-} (366 cm^{-1}), the asymmetric stretching mode of V-O bonds (640 and 710 cm^{-1}) and the symmetric stretching mode of V-O bonds (830 cm^{-1}) [7,15]. As shown in Fig. 2(A), BVO1 and BVO2 samples exhibited all Raman signals corresponding to monoclinic phase. Furthermore, no Raman signals corresponding to bismuth oxides or vanadium oxides was observed in these samples, which is consistent with the results of XRD patterns. For BVO3 sample, however, the peak appeared at 506 cm^{-1} was attributed to NaV_6O_{15} phase due to the excess of V content. In addition, the V–O bond length can be calculated using the empirical expression: $\nu\ [cm^{-1}] = 21{,}349*\exp(-1.9176R\ [Å])$ [16], wherein ν and R are the Raman shift and the bond length, respectively. The transition of the ν_s(V-O) band shift of BVO1, BVO2 and BVO3 sample are 835.47, 833.98 and 835.47 cm^{-1}, respectively. The V–O bond lengths in BVO1, BVO2 and BVO3 were calculated to have 1.690, 1.692 and 1.69 Å, respectively.

As shown in Fig. 2(B), we can observe the transition of the ν_s(V-O) band shift of BVO4 and BVO5 samples at 833.98, 818.05 and 830.49 cm^{-1}, respectively. In addition, the V–O bond lengths in BVO4 and BVO5 were obtained to have 1.700 and 1.691 Å. This result indicates that the BVO4 sample has a tetragonal scheelite phase, while BVO2 and BVO5 samples show to have a monoclinic scheelite phase owing to that the band corresponding to symmetric V–O stretching mode in m-s $BiVO_4$ (BVO2 and BVO5) shifts toward higher wavenumber (the V–O bond length decreases) compared to s-t $BiVO_4$ (BVO4). From the XRD data and Raman spectra, the monoclinic scheelite phase $BiVO_4$ sample can be obtained at higher solvothermal synthesis temperature more than 140 °C.

Preprints (www.preprints.org) | NOT PEER-REVIEWED | Posted: 12 June 2018 doi:10.20944/preprints201806.0199.v1

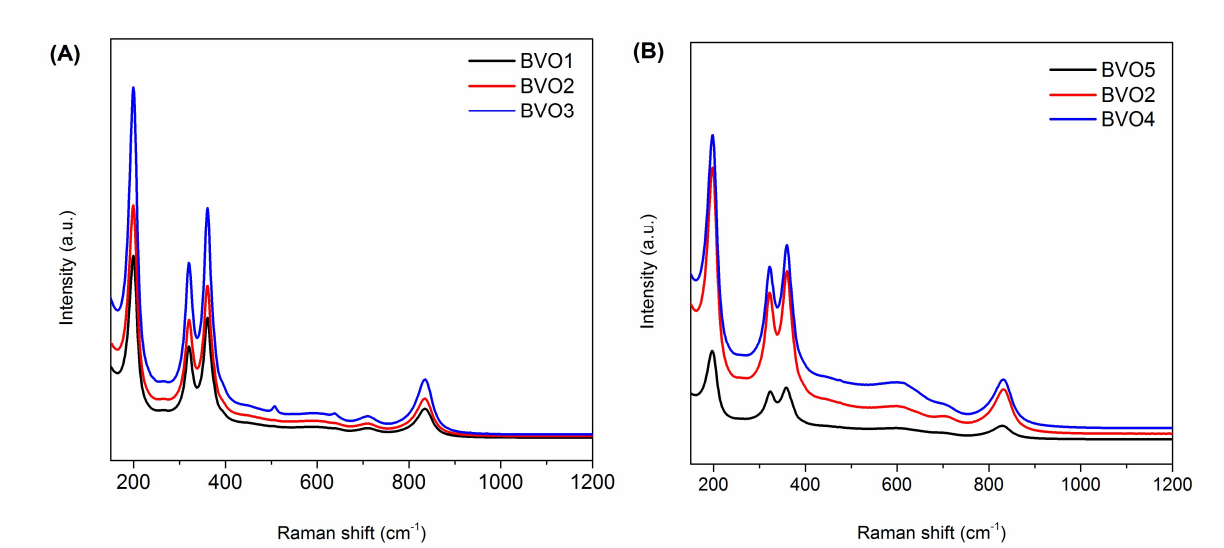

Fig. 2. Raman spectra of $BiVO_4$ samples prepared using different Bi/V molar ratio (A) and different synthesis temperature (B).

Fig. 3 shows the SEM images of $BiVO_4$ samples, which were prepared using different Bi/V molar ratio and different synthesis temperature. As shown in Fig. 3, the morphologies and shapes of $BiVO_4$ samples varied according to the Bi/V molar ratio and synthesis temperature. This result was conceded that the morphology of $BiVO_4$ is dependent on the preparation conditions.

When $BiVO_4$ sample was prepared at the Bi/V molar ratio= 1/1 (BVO1), the product exhibited ellipsoidal shape morphology with a diameter of about 0.53 ± 0.09 µm. The $BiVO_4$ sample was prepared in the excess bismuth (BVO2) led to the formation of needle-like morphology with 1.52 ± 0.15 µm in length. When the $BiVO_4$ sample was prepared in the excess vanadium (BVO3), however, the mixture of spherical and rods shape was observed (Fig. 3(C)).

As shown in Fig. 3(D) and (E), the synthesis temperature also played an important role on the morphologies of $BiVO_4$ samples. When $BiVO_4$ sample was prepared at lower temperature (BVO4), non-uniform needle-like morphology of $BiVO_4$ was observed. In addition, when $BiVO_4$ sample was prepared at 180 ^oC (BVO5), $BiVO_4$ sample with a mixture of ellipsoidal and rod morphology was obtained. This result suggests that the preparation conditions such as, the Bi/V molar ratio and synthesis temperature, have significantly effects on the morphologies of the $BiVO_4$ samples.

Preprints (www.preprints.org) | NOT PEER-REVIEWED | Posted: 12 June 2018 doi:10.20944/preprints201806.0199.v1

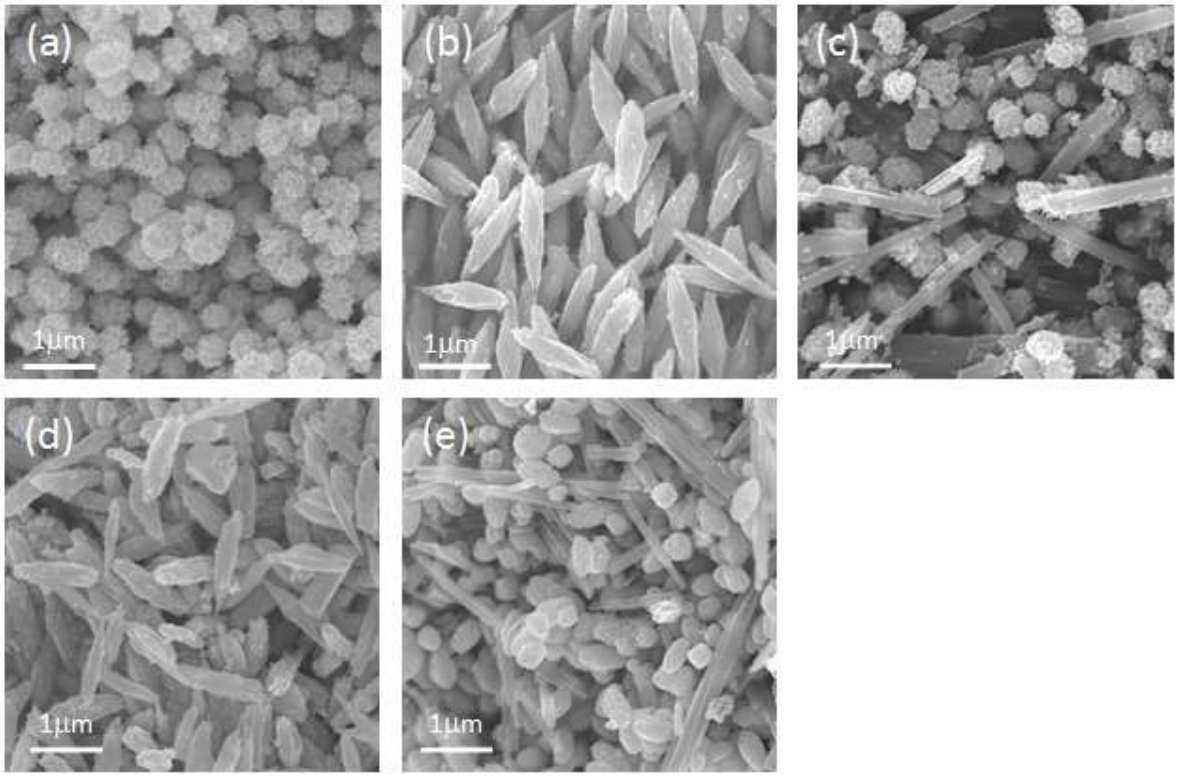

Fig. 3. SEM images of $BiVO_4$ samples prepared using different Bi/V molar ratio and different synthesis temperature: a) BVO1, b) BVO2, c) BVO3, d) BVO4 and e) BVO5.

The light absorption properties of photocatalysts were examined in DRS. Fig. 4 shows the DRS spectra of as-prepared $BiVO_4$ samples, which were prepared using different Bi/V molar ratio(A) and different synthesis temperature(B). As shown in Fig. 4, all the catalysts displayed strong absorption in the visible range of the electromagnetic spectrum. Owing to the absorbance of visible light, the photocatalytic property of $BiVO_4$ materials was enhanced in the visible region of electromagnetic spectrum. The indirect band gap energy (E_g) of all the samples was calculated from the tangent lines obtained in the plots of modified Kubelka–Munk function $[F(R'_\infty)h\vartheta]^{1/2}$ versus photon energy. The band gap values of various $BiVO_4$ samples are presented in Table 1. As shown in Table 1, the estimated band gap values of $BiVO_4$ samples are obtained in the range of 2.34 – 2.43 eV.

Preprints (www.preprints.org) | NOT PEER-REVIEWED | Posted: 12 June 2018 doi:10.20944/preprints201806.0199.v1

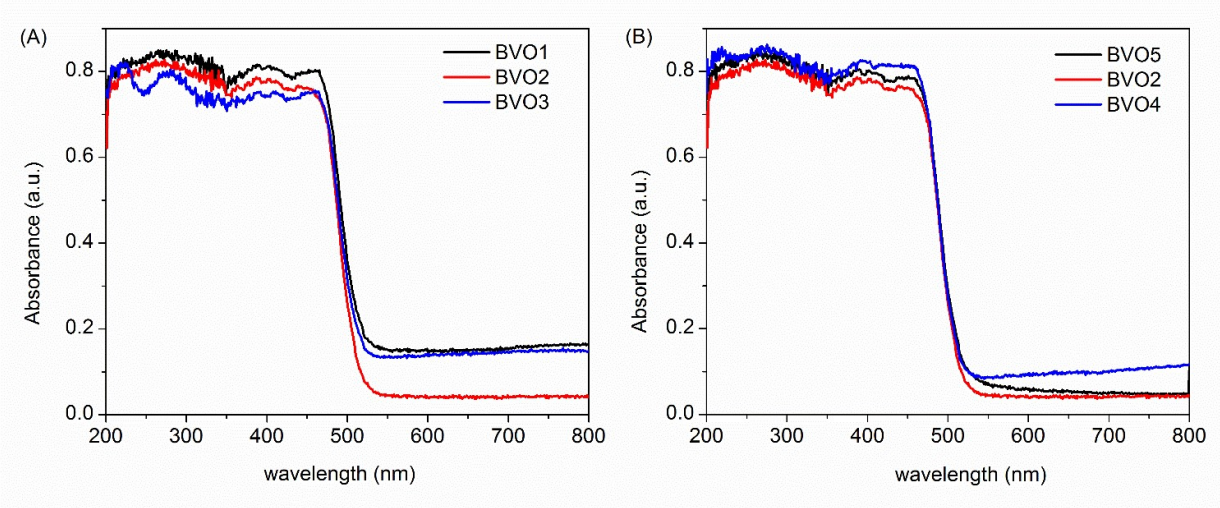

Fig. 4. UV-vis spectra of $BiVO_4$ samples prepared using different Bi/V molar ratio (A) and different synthesis temperature (B).

Table 1. The physical properties and photocatalytic activity of $BiVO_4$ samples.

Sample	$E_{band\ gap}$ (eV)	k'(x10^{-3}min^{-1})
BVO1	2.37	9.0
BVO2	2.43	42.8
BVO3	2.39	4.0
BVO4	2.36	1.0
BVO5	2.34	30.0

The PL emission spectrum excited at 315 nm of terephthalic acid solution was measured under visible light irradiation. Fig. 5 shows the changes of PL spectra of terephthalic acid solution with 1 h visible light irradiation time on the BiVO4 samples prepared using different Bi/V molar ratio. As shown in Fig. 5, no photoluminescence signal was observed in the absence of photocatalyst. However, for the BVO1, BVO2 and BVO3 samples, a blue emission signal at approximately 425 nm was observed. This result suggests that the signal of PL is only caused 2-hydroxyterephthalic acid obtained by the reaction of terephthalic acid with the OH radical formed on the interface of the photocatalyst/water during visible light irradiation. The PL peak of BVO2 sample shows the highest

Preprints (www.preprints.org) | NOT PEER-REVIEWED | Posted: 12 June 2018 doi:10.20944/preprints201806.0199.v1

intensity among of all $BiVO_4$ samples. The formation rate of OH radicals shows a good correlation with the photocatalytic activity.

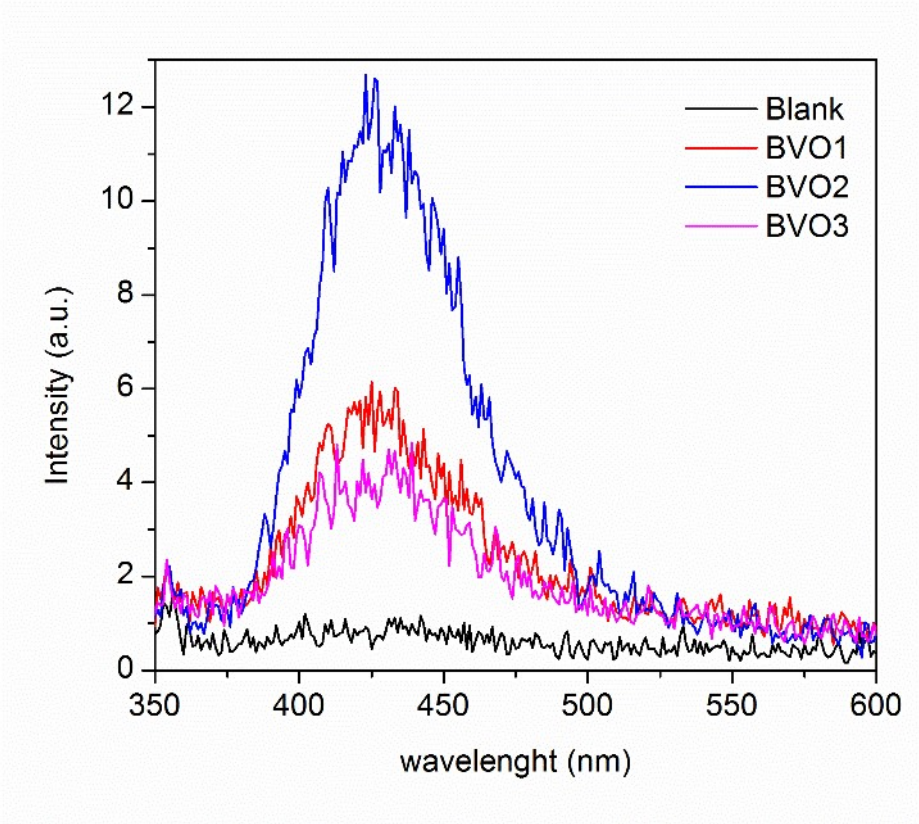

Fig. 5. Fluorescence emission spectra of $BiVO_4$ samples prepared using different Bi/V molar ratio in the presence of terephthalic acid.

3.2. Photocatalytic test

In order to evaluate the photocatalytic activities of the as-synthesized $BiVO_4$ samples, we investigated the degradation ability of RhB dye in water in the presence of visible light. Fig. 6 shows the temporal evolution of the UV-vis spectra produced by the photodegradation of RhB dye. In this reaction, $BiVO_4$ sample prepared at Bi/V molar ratio=1/1(BVO2) was used as the photocatalyst in the presence of visible light ($\lambda > 400$ nm). As seen in the above spectra, the absorption of RhB/$BiVO_4$ sample and suspensions gradually decreased during the photodegradation process. In addition, the major absorption peak, which corresponds to RhB, was shifted from 554 to 500 nm in a step-wise manner. Thus, the ethyl groups were removed one by one in this reaction. This finding is in good

Preprints (www.preprints.org) | NOT PEER-REVIEWED | Posted: 12 June 2018 doi:10.20944/preprints201806.0199.v1

agreement with the previous literature [17].

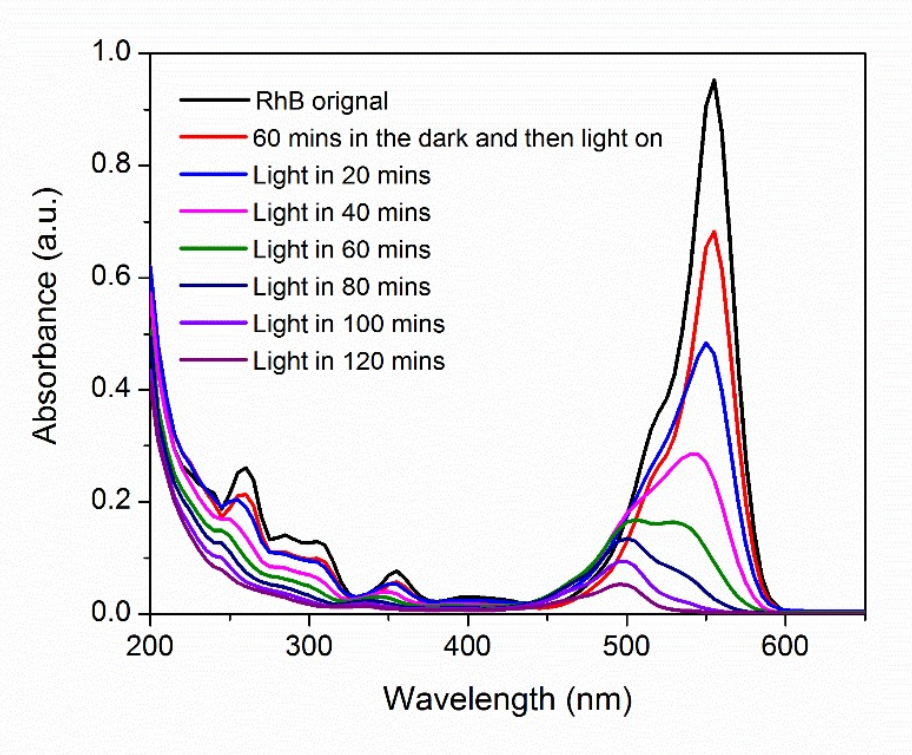

Fig. 6. UV-vis absorption spectra of RhB solution separated from catalyst suspension during illumination using BVO2 sample.

It is a well-known fact that the photocatalytic oxidation of organic pollutants follows Langmuir-Hinshelwood kinetics [18], where the rate is proportional to the coverage θ:

$$r = -\frac{dc}{dt} = k\theta = k\frac{KC}{1+KC} \qquad (1)$$

Here, k is the true rate constant; it is dependent upon various parameters, such as the mass of the catalyst, the flux efficiency, and oxygen coverage. K is the adsorption coefficient of the reactant, and C is the concentration of the reactant. When C is very small, the product KC is negligible with respect to unity. Under these conditions, Eq. (1) represents a first-order kinetic reaction. When the parameters of Eq. (1) are set to the initial conditions of a photocatalytic procedure, $t = 0$ and the concentration can be given as $C=C_0$. Substituting these initial values of reactions in Eq. (1), we obtain Eq. (2) as follows;

Preprints (www.preprints.org) | NOT PEER-REVIEWED | Posted: 12 June 2018 doi:10.20944/preprints201806.0199.v1

$$-ln\left(\frac{C}{Co}\right) = k_{app}t \qquad (2)$$

where k_{app} is the apparent first-order reaction constant

In Fig. 7 and Table 1, we have presented how visible light influences the photocatalytic activity associated with the decomposition of RhB over $BiVO_4$ samples, which were prepared using different Bi/V molar ratio(A) and different synthesis temperature(B). When a blank test was carried out in the absence of the photocatalyst, about 7% of the RhB was decomposed after 2 h by the photolysis reaction.

As shown in Fig. 7, $BiVO_4$ sample prepared at Bi/V molar ratio=2/1(BVO2) shows the highest photocatalytic activity in the photodegradation of RhB under visible light irradiation. The k value of BVO2 catalyst was 42.8 × 10^{-3} min^{-1}, which is much higher than that of $BiVO_4$ samples prepared different Bi/V molar ratio. However, BVO4 sample shows the lowest photocatalytic activity, even though it was prepared with the same Bi/V molar ratio and similar morphology with BVO2 sample. It is thought that BVO4 sample possesses the tetragonal scheelite phase, which is known to have low photocatalytic activity on the decomposition of organic dyes.

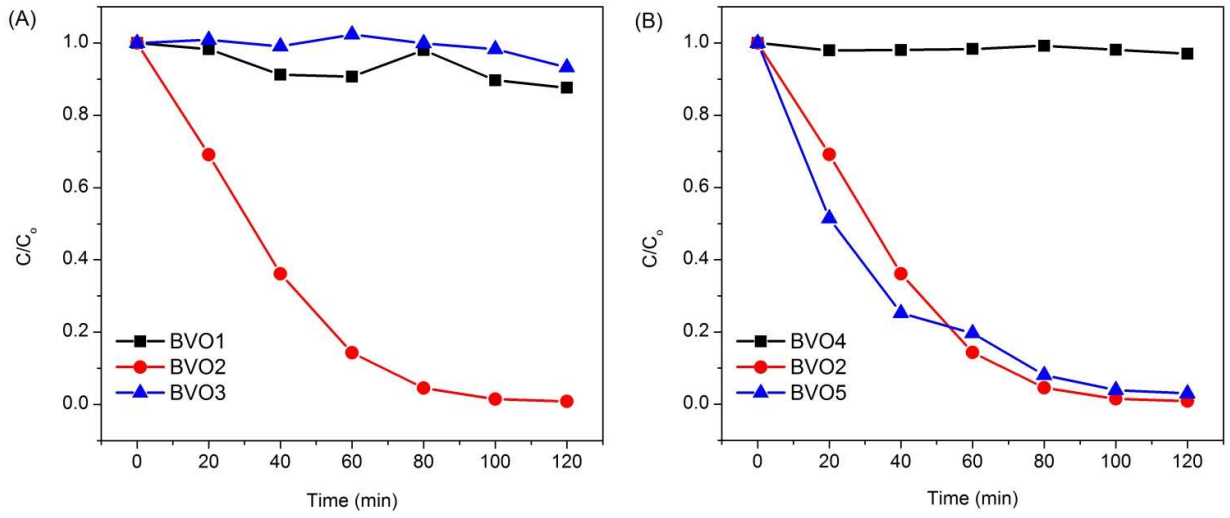

Fig. 7. Photocatalytic decomposition of RhB over $BiVO_4$ samples prepared using different Bi/V molar ratio (A) and different synthesis temperature (B).

 doi:10.20944/preprints201806.0199.v1

It is well known that OH radical plays an important role on the photocatalytic decomposition of organic dyes [13]. Generally, the greater the formation rate of OH radicals is, the higher separation efficiency of electron-hole pairs is achieved. Therefore, the photocatalytic activity is in positive correlation to the formation rate of OH radicals, namely, a faster formation rate of OH radicals leads to a higher photocatalytic activity. As shown in Fig. 5, BVO2 sample shows the highest PL peak, which has the highest formation rate of OH radicals and the highest photocatalytic activity. This result suggests that the formation rate of OH radicals shows a good correlation with the photocatalytic activity.

4. Conclusion

A highly crystallized monoclinic-scheelite type $BiVO_4$ powders were successfully synthesized by solvothermal method from bismuth neodecanoate and ammonium metavanadate solutions in water-ethanol media, combined with the introduction of oleic acid as surfactant. The physical properties of the synthesized $BiVO_4$ powders were investigated by XRD, FE-SEM, Raman spectroscopy, UV-vis DRS spectroscopy and TA-PL. From the XRD data and Raman spectra, the monoclinic scheelite phase $BiVO_4$ sample can be obtained at higher solvothermal synthesis temperature more than 140 ^oC. The preparation conditions such as, the Bi/V molar ratio and synthesis temperature, have significantly effects on the morphologies of the $BiVO_4$ samples. BVO2 sample shows the highest PL peak, which has the highest formation rate of OH radicals and the highest photocatalytic activity. This result suggests that the formation rate of OH radicals shows a good correlation with the photocatalytic activity.

.

References

1. Ye, L.; Su, Y.; Jin, X.; Xie, H; Zhang, C. Recent advances in BiOX (X = Cl, Br and I) photocatalysts: synthesis, modification, facet effects and mechanisms. *Environ. Sci. Nano* **2014**, *1*, 90-112.

2. Sun, S; Wang, W. Advanced chemical compositions and nanoarchitectures of bismuth based complex oxides for solar photocatalytic application. *RSC Adv*. **2014**, *4*, 47136-47152.

3. Park, Y.; McDonald, K.J.; Choi, K.-S. Progress in bismuth vanadate photoanodes for use in solar water oxidation. *Chem. Soc. Rev.* **2013**, 2321-2337.

4. Liu, Y.; Huang, B.; Dai, Y.; Zhang, X.; Qin, X.; Jiang, M.; Whangbo M. H. Selective ethanol formation from photocatalytic reduction of carbon dioxide in water with BiVO4 photocatalyst. *Catal. Commun*. **2009**,*11,* 210-213.

5. Mao, J.; Peng, T.; Zhang, X.; Li, K.; Zan, L. Selective methanol production from photocatalytic reduction of CO_2 on $BiVO_4$ under visible light irradiation. *Catal. Commun*. **2012** , *28*, 38-41.

6. Lim, A.R.; Choh, S.H.; Jang, M.S. Prominent ferroelastic domain walls in $BiVO_4$ crystal. *J. Physics-Condensed Matter.* **1995**, *7*, 7309-7323.

7. Yu, J.; Kudo, A. Effects of structural variation on the photocatalytic performance of hydrothermally synthesized $BiVO_4$. *Adv. Funct. Mater.* **2006**, *16*, 2163-2169.

8. Yang, T.; Xia, D.; Chen, G.; Chen, Y. Influence of the surfactant and temperature on the morphology and physico-chemical properties of hydrothermally synthesized composite oxide $BiVO_4$. *Mater. Chem. Phys.* **2009**, *114*, 69-72.

9. Obregon, S.; Caballero, A.; Colon, G. Hydrothermal synthesis of $BiVO_4$: Structural and morphological influence on the photocatalytic activity. *Appl. Catal. B-Environmental* **2012**, *112,* 59-66.

10. Xi, G.; Ye, J. Synthesis of bismuth vanadate nanoplates with exposed {001} facets and enhanced visible-light photocatalytic properties. *Chem. Commun*. **2010**, *46*, 1893-1895

11. Wang, D.; Jiang, H.; Zong, X.; Xu, Q.; Ma, Y.; Li, G.; Li, C. Crystal facet dependence of water oxidation on $BiVO_4$ sheets under visible light irradiation. *Chem. - A Eur. J.* **2011**, *17*, 1275-1282.

12. Yu, J.; Wang, W.; Cheng, B.; Su, B.L. Enhancement of photocatalytic activity of mesporous TiO_2 powders by hydrothermal surface fluorination treatment. *J. Phys. Chem. C* **2009**, *113*, 6743-6750.

13. Hu, Y.; Li, D.; Sun, F.; Wang, H.; Weng, Y.; Xiong, W.; Shao, Y. One-pot template-free synthesis of heterophase $BiVO_4$ microspheres with enhanced photocatalytic activity. *RSC Adv*. **2015**, *5*, 54882-54889.

14. Tokunaga, S.; Kato, H.; Kudo, A. Selective preparation of monoclinic and tetragonal $BiVO_4$ with scheelite structure and their photocatalytic properties. *Chem. Mater.* **2001**, *13*, 4624-4628.

15. Frost, R.L.; Henry, D.A.; Weier, M.L.; Martens, W. Raman spectroscopy of three polymorphs of $BiVO_4$: clinobisvanite, dreyerite and pucherite, with comparisons to $(VO_4)^3$-bearing minerals:

 doi:10.20944/preprints201806.0199.v1

namibite, pottsite and schumacherite. *J. Raman Spectrosc.* **2006**, *37*, 722-732.

16. Brown, I.D.; Wu, K.K. Empirical parameters for calculating cation–oxygen bond valences. *Acta Crystallogr. Sect. B Struct. Crystallogr. Cryst. Chem.* **1976**, *32*, 1957-1959.

17. Nguyen, D.T.; Hong, S.S. Synthesis of $BiVO_4$ nanoparticles using microwave process and their photocatalytic activity under visible light irradiation, *J. Nanosci. Nanotech*. **2017**, *17*, 2690-2694.

18. Jung, W.Y.; Hong, S.S. Photocatalytic decomposition of methylene blue over yttrium ion doped Ti-SBA-15 catalysts *Catal. Today*, **2011**, *164*, 395-398.